NUMERICAL ANALYSIS OF ACOUSTIC WAVE GENERATION IN ANISOTROPIC PIEZOELECTRIC MATERIALS*

ERASMUS LANGER and SIEGFRIED SELBERHERR

Department of Physical Electronics, Technical University of Vienna (Austria)

PETER A. MARKOWICH and CHRISTIAN A. RINGHOFER**

Department of Applied Mathematics, Technical University of Vienna (Austria)

Abstract

We present an *ab initio* transient analysis of acoustic wave generation in piezoelectric materials, which takes into account second-order effects (*e.g.*, bulk wave generation and interaction between surface waves and bulk waves). The computer program we have developed for this purpose solves the fundamental differential equations in two space dimensions with the corresponding mechanical displacements and the electrical potential as dependent variables using a semi-implicit finite difference scheme rather than by wave approximations. This has become possible with acceptable usage of computer resources only by introducing a novel form of boundary conditions for the quasi-infinite sagittal plane to avoid reflection phenomena. We present numerical results for YZ $LiNbO_3$.

1. Introduction

There are many publications dealing with surface acoustic wave propagation, but either the authors *a priori* postulate a wave approximation [1, 2] or simulate an infinite periodic structure [3]. Our method is different since we do not anticipate the solution in any way. We solve the fundamental equations in two space dimensions — in the sagittal plane — by a semi-implicit time integration scheme using a novel form of boundary conditions for the quasi-infinite domain. Therefore, we can correctly analyse the excitation of surface and bulk waves simply by considering a relatively small area below the electrodes of the transducer. The input data for our program are the geometry of the transducer fingers, the substrate material and the Euler's angles of the crystal cut. The structure and the actual values of the material-dependent tensors are stored in a database for most of the common materials.

*Based on a Paper presented at Solid-State Transducers 83, Delft, The Netherlands, May 31 - June 3, 1983.

**Present address: Mathematics Research Center, University of Wisconsin, Madison, U.S.A.

0250-6874/83/$3.00 © Elsevier Sequoia/Printed in The Netherlands

However, the analysis of new materials is merely a matter of specifying the tensor data. One major objective of our investigation is the quest for physical insight into SAW devices to enable simple analytic formulae for device characterization and design to be developed. The power of our analysis method is twofold. First, it lies in the general applicability with respect to different materials and crystal cuts and, secondly, the interaction between surface waves and bulk waves is not neglected. For these reasons our computer program can be used, for instance, to optimize a crystal cut by minimizing the acoustic power radiation in the bulk. Because of the chosen solution method the program could be extended to include non-linearity effects. In this paper the transient behaviour of a transducer structure with four fingers is demonstrated for the YZ cut of $LiNbO_3$.

2. The physical and mathematical model

The physical model is based on the fundamental set of equations describing acoustic wave propagation in an arbitrary piezoelectric material consisting of equations of motion (1), the linear, strain-mechanical displacement relations (2), Maxwell's equations under the quasi-static assumptions (3, 4) and the linear piezoelectric constitutive relations (5, 6) [4]. It is to be noted that standard tensor notation as well as Einstein's summation convention is used.

$$\frac{\partial T_{ij}}{\partial x_i} = \frac{\rho \partial^2 u_j}{\partial t^2} \tag{1}$$

$$S_{kl} = \left(\frac{\partial u_k}{\partial x_l} + \frac{\partial u_l}{\partial x_k}\right) \Big/ 2 \tag{2}$$

$$\frac{\partial D_l}{\partial x_l} = 0 \tag{3}$$

$$E_l = -\frac{\partial \phi}{\partial x_l} \tag{4}$$

$$T_{ij} = c_{ijkl} S_{kl} - e_{nij} E_n \tag{5}$$

$$D_m = e_{mkl} S_{kl} + \mathrm{E}_{mn} E_n \tag{6}$$

T denotes the stress, ρ the mass density, u the mechanical displacement, S the strain, D the electric displacement, E the electric field, ϕ the electric potential. The fourth rank tensor c is the elastic stiffness tensor, the third rank tensor e the piezoelectric tensor, and the second rank tensor E the dielectric tensor in the actual, *i.e.*, rotated coordinate system. These three tensors are the result (7, 8, 9) of a transformation of the unrotated quantities c^0, e^0, and E^0 according to Euler's transformation matrix V:

$$c_{ijkl} = V_{ir}V_{js}V_{kt}V_{lq}c^0{}_{rstq} \tag{7}$$

$$e_{ijk} = V_{ir}V_{js}V_{kt}e^0{}_{rst} \tag{8}$$

$$\mathrm{E}_{ij} = V_{ir}V_{js}\mathrm{E}^0_{rs} \tag{9}$$

By substituting eqns. (2) and (4) into eqns. (5) and (6) and then eliminating the mechanical stress T and the electric displacement D, one obtains a system of partial differential equations in three space dimensions ($j = 1, 2, 3$) which consists of three mechanical wave equations (10) and Poisson's equation (11):

$$c_{ijkl}\ \frac{\partial^2 u_k}{\partial x_l \partial x_i} - e_{kij}\ \frac{\partial^2 \phi}{\partial x_k\, \partial x_i} = \frac{\rho \partial^2 u_j}{\partial t^2} \tag{10}$$

$$e_{ikl}\ \frac{\partial^2 u_k}{\partial x_l \partial x_i} - \mathrm{E}_{ik}\ \frac{\partial^2 \phi}{\partial x_k\, \partial x_i} = 0 \tag{11}$$

The surface boundary conditions for the mechanical quantities result from the fact that the force component perpendicular to the surface plane vanishes, *i.e.*, $T_{3j} = 0$ ($j = 1, 2, 3$). For Poisson's equation the surface boundary condition is derived from the fact that the electrical displacement D_3 vanishes.

Assuming the finger length to be much larger than the finger width, we can reduce the system to the two space dimensions, $x = x_1$ and $z = x_3$. The solution vector s is defined with its components u, v, w (mechanical displacement components) and ϕ (electric potential). This procedure leads to the following set of equations and the surface boundary condition:

$$\mathbf{A}s_{xx} + \mathbf{B}s_{xz} + \mathbf{C}s_{zz} = \Omega s_{tt}, \qquad t > 0, \qquad x \in R, \qquad z < 0 \tag{13}$$

$$\mathbf{F}s_x + \mathbf{G}s_z = 0 \tag{14}$$

A, **B**, **C**, **F**, **G** are 4×4 matrices and **A**, **B**, **C**, **G** are symmetric. Ω is a diagonal matrix whose main diagonal has the entries $\rho, \rho, \rho, 0$. The boundary condition (14) holds for the mechanical equations for all $x \in R$ and for the fourth (ϕ) equation on the free surface and $\phi = V_i(t)$ on the ith finger.

Artificial boundaries have to be introduced in the sagittal plane in order to obtain a finite-dimensional linear system of equations with (13) and the discrete boundary conditions at the surface for each time step. The obvious way to do this is to solve eqn. (13) in a rectangle (which includes all fingers) and to impose zero Neumann or Dirichlet boundary conditions at those boundaries of the rectangle which do not coincide with the surface. This approach, however, leads to reflections as soon as a wave hits the artificial boundary and therefore has to be abandoned. The method of transformation of the infinite sagittal plane into finite subdomains [5] has the drawback of relatively large discretization errors in these domains.

Our new method is based on the fact that at a sufficiently large distance from the fingers there exist only plane bulk waves with approximately radial propagation direction. First we transform eqn. (13) into polar coordinates

(α, r) and form the limiting value for r to infinity. This yields a system of partial differential equations in one dimension which has the mentioned plane waves as solutions:

$$\mathrm{H}s_{rr} = \Omega s_{tt} \tag{15}$$

where $\mathrm{H} = \mathrm{A}\cos^2\alpha + \mathrm{B}\cos\alpha\sin\alpha + \mathrm{C}\sin^2\alpha$

$$s_r = s_x\cos\alpha + s_z\sin\alpha = -\sqrt{\mathrm{H}^{-1}\Omega}\,s_t \tag{16}$$

The boundary condition (16), which is a generalized form of Sommerfeld's radiation condition, satisfies the equation system (15) implicitly and, therefore, absorbs all possible radial plane waves.

The numerical solution method and especially the discretization used can be found in ref. 5. At each time step the mechanical quantities on the inner grid points are calculated explicitly from the known values at the two previous time steps, whereas the unknowns on all boundaries as well as the complete distribution of the electric potential have to be solved fully implicitly. To solve the large linear equation system at each time step we use a so called 'Line SOR' iterative method similar to that used in the program package ITPACK [6].

The main advantage of the described difference method compared to the frequently-used Fourier transform method is that the difference method can easily be applied to non-linear elasticy laws, while the Fourier method relies strictly on the linearity of the problem.

3. Results

We present a transient analysis of a four finger transducer structure for Y-cut Z-propagating $LiNbO_3$. The distance between two neighbouring electrodes as well as the finger width amounts to 250 μm. As described in the previous section, we analyse the propagation phenomena in the sagittal plane. The applied voltage on the electrodes is a sinusoidal function in time with a horizontal tangent at $t = 0$ to get consistent initial values. After a quarter period the voltage is a sine function with an amplitude of 0.5 V. As we are mostly interested in surface waves, we take the corresponding resonance frequency of 3.5 MHz. It should be mentioned that in the following Figures the unit of length is metres both for the geometry and the mechanical displacement.

Figure 1 shows the mechanical displacement component u (which is the component parallel to the surface) after $1\frac{1}{2}$ periods in a quasi three-dimensional plot. The rectangular bottom of the drawing is the sagittal plane, whereas the third dimension represents the dependent variable (pay attention to the scale factor on the right boundary). One can clearly see that the displacement has its maximum on the surface and decays rapidly in the direction of the bulk. At this time the surface wave just hits the artificial boundaries.

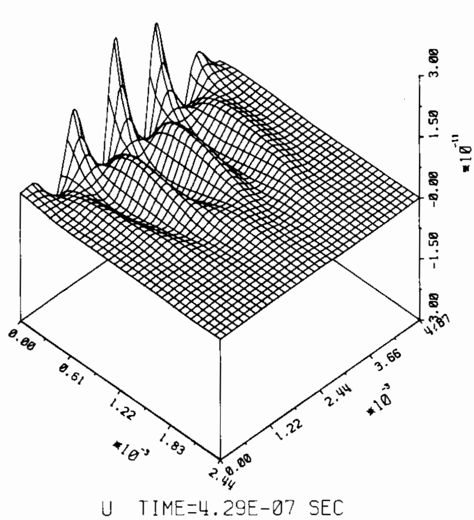

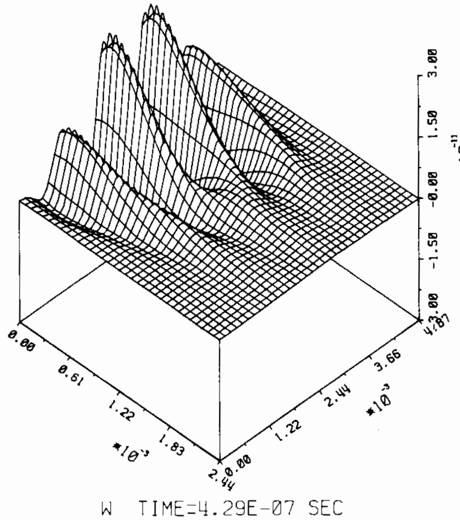

Fig. 1. Displacement component u after $1\frac{1}{2}$ periods.

Fig. 2. Displacement component w after $1\frac{1}{2}$ periods.

Figure 2 shows the mechanical displacement component w (which is the component perpendicular to the surface) in the same representation and at the same time as Fig. 1. The depth dependence is quite different compared to the component u. The maximum lies below and not in the surface and the decrease into the bulk is slower.

Figure 3 shows the electric potential distribution in volts corresponding to Figs. 1 and 2. At this time the applied voltage on all electrodes is zero, so that this plot represents the mechanical–electrical reaction. Because of the

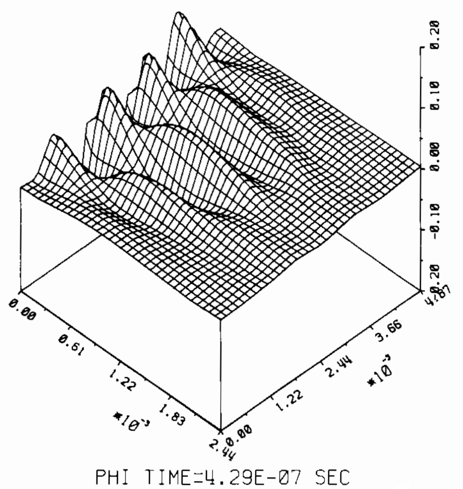

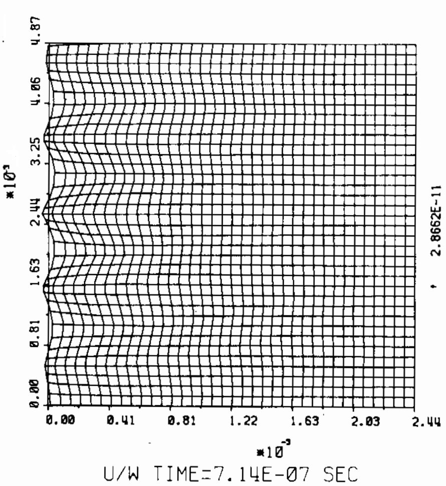

Fig. 3. Electric potential after $1\frac{1}{2}$ periods.

Fig. 4. Distortion in the sagittal plane after $2\frac{1}{2}$ periods.

zero voltage applied at this time, one can clearly identify the location of the fingers.

It is to be noted that for this special cut of $LiNbO_3$, the second equation of the equation set (13) as well as the second equation of the boundary conditions (14) are totally decoupled from the others. In this case, therefore, the mechanical displacement component v is not relevant for wave propagation.

Figure 4 shows a distortion plot of the sagittal plane after $2\frac{1}{2}$ periods. This representation includes both relevant displacement components u and w. The left vertical boundary represents the surface. Note the unit vector on the right boundary of the figure. At this time, the front of the surface wave has already passed through the artificial boundary. The plot clearly demonstrates that the surface wave consists of a transverse as well as a longitudinal component.

Acknowledgement

This work is supported by the Fonds zur Förderung der wissenschaftlichen Forschung (Projekt Nr. S22/11) and by Siemens AG, Munich.

References

1 R. F. Milsom, N. H. C. Reilly and M. Redwood, Analysis of generation and detection of surface and bulk acoustic waves by interdigital transducers, *IEEE Trans. Sonics and Ultrasonics, SU-24* (May 1977) 147.
2 R. Peach, A general approach to the electrostatic problem of the SAW interdigital transducer, *IEEE Trans. Sonics and Ultrasonics, SU-28* (March 1981) 96.
3 Y. Kagawa and T. Yamabuchi, A finite element approach to electromechanical problems with an application to energy-trapped and surface-wave devices, *IEEE Trans. Sonics and Ultrasonics, SU-23* (July 1976) 263.
4 B. A. Auld, *Acoustic Fields and Waves in Solids*, John Wiley, New York, 1973.
5 E. Langer, S. Selberherr, P. A. Markowich and Ch. A. Ringhofer, Numerical analysis of generation of acoustic waves in anisotropic piezoelectric materials, *Proc. Ultrasonics Symposium, San Diego, California, USA, Oct. 1982*, pp. 350.
6 R. G. Grimes, D. R. Kincaid and D. M. Young, *ITPACK 2A — A Fortran implementation of adaptive accelerated iterative methods for solving large sparse linear systems*, Center for Numerical Analysis, University of Texas at Austin, Oct. 1980.